European Radiology (2019) 29:2802–2811
https://doi.org/10.1007/s00330-018-5787-2

MAGNETIC RESONANCE

Predicting the grade of hepatocellular carcinoma based on non-contrast-enhanced MRI radiomics signature

Minghui Wu[1] · Hongna Tan[1] · Fei Gao[2] · Jinjin Hai[2] · Peigang Ning[1] · Jian Chen[2] · Shaocheng Zhu[1] · Meiyun Wang[1] · Shewei Dou[1] · Dapeng Shi[1]

Received: 30 May 2018 / Revised: 1 September 2018 / Accepted: 21 September 2018 / Published online: 7 November 2018

Abstract

Purpose This study was conducted in order to investigate the value of magnetic resonance imaging (MRI)-based radiomics signatures for the preoperative prediction of hepatocellular carcinoma (HCC) grade.

Methods Data from 170 patients confirmed to have HCC by surgical pathology were divided into a training group ($n = 125$) and a test group ($n = 45$). The radiomics features of tumours based on both T1-weighted imaging (WI) and T2WI were extracted by using Matrix Laboratory (MATLAB), and radiomics signatures were generated using the least absolute shrinkage and selection operator (LASSO) logistic regression model. The predicted values of pathological HCC grades using radiomics signatures, clinical factors (including age, sex, tumour size, alpha fetoprotein (AFP) level, history of hepatitis B, hepatocirrhosis, portal vein tumour thrombosis, portal hypertension and pseudocapsule) and the combined models were assessed.

Results Radiomics signatures could successfully categorise high-grade and low-grade HCC cases ($p < 0.05$) in both the training and test datasets. Regarding the performances of clinical factors, radiomics signatures and the combined clinical and radiomics signature (from the combined T1WI and T2WI images) models for HCC grading prediction, the areas under the curve (AUCs) were 0.600, 0.742 and 0.800 in the test datasets, respectively. Both the AFP level and radiomics signature were independent predictors of HCC grade ($p < 0.05$).

Conclusions Radiomics signatures may be important for discriminating high-grade and low-grade HCC cases. The combination of the radiomics signatures with clinical factors may be helpful for the preoperative prediction of HCC grade.

Key Points

- *The radiomics signature based on non-contrast-enhanced MR images was significantly associated with the pathological grade of HCC.*
- *The radiomics signatures based on T1WI or T2WI images performed similarly at predicting the pathological grade of HCC.*
- *Combining the radiomics signature and clinical factors (including age, sex, tumour size, AFP level, history of hepatitis B, hepatocirrhosis, portal vein tumour thrombosis, portal hypertension and pseudocapsule) may be helpful for the preoperative prediction of HCC grade.*

Keywords Hepatocellular carcinoma · Magnetic resonance imaging · Diagnostic imaging · ROC curve

Abbreviations

3D	Three-dimensional
AFP	Alpha fetoprotein
AUC	Area under the curve
CHB	Chronic hepatitis B
CI	Confidence interval
DWI	Diffusion-weighted imaging
GLCM	Grey-level co-occurrence matrix
GLN	Grey-level run-length non-uniformity
GLRLM	Grey-level run-length matrix
HCC	Hepatocellular carcinoma
LASSO	Least absolute shrinkage and selection operator

Electronic supplementary material The online version of this article (https://doi.org/10.1007/s00330-018-5787-2) contains supplementary material, which is available to authorized users.

✉ Dapeng Shi
cjr.shidapeng@vip.163.com

[1] Radiological Department of the People's Hospital of Zhengzhou University and Henan Provincial People's Hospital, No. 7 Weiwu Road, Zhengzhou 450003, Henan, China

[2] National Digital Switching System Engineering and Technological R&D Center, Zhengzhou 450002, Henan, China

MRI	Magnetic resonance imaging
MVI	Microvascular invasion
NSCLC	Non-small cell lung cancer
OR	Odds ratio
PACS	Picture archiving and communication system
ROC	Receiver operating characteristic
ROI	Region of interest
T1WI	T1-weighted imaging
T2WI	T2-weighted imaging
TE	Echo time
TR	Repetition time

Introduction

Hepatocellular carcinoma (HCC) is now the most common malignant tumour and the second leading cancer-related cause of death worldwide [1–3]. Clinically, HCC is prone to metastasis and recurrence, and its prognosis is very poor. Pathological grading is one of the factors that influence intrahepatic recurrence [4], and high-grade HCC tumours have a higher rate of intrahepatic recurrence than low-grade tumours [5]. Most patients with high-grade HCC tumours are reportedly at high risk of recurrence and need large safety margins at surgical resection, frequent posttreatment follow-up examinations or both, whereas patients with low-grade HCC have lower risk of recurrence [6, 7]. Therefore, accurate prediction of the HCC grade before treatment might facilitate the selection of treatment strategy.

Radiomics is an emerging research field that aims to utilise the full potential of medical images [8], and it can be used for high-throughput extraction of quantitative features, such as shape, greyness, texture and wavelet, from medical images [9, 10]. Radiomics signatures have been proven to reflect tissue heterogeneity [11–16]. Computed tomography (CT)-based texture analysis has been used to predict tumour grade in both oesophageal cancer and non-small cell lung cancer (NSCLC) [17, 18], and the combined analysis of multiple predictors has been regarded as a powerful method to assist tumour grading [19].

Medical imaging plays an important role in the diagnosis of HCC [20]. Magnetic resonance imaging (MRI) has been used widely for the detection and assessment of HCC. MRI with a liver-specific contrast agent and diffusion-weighted imaging (DWI) have been shown to be helpful in assessing the histological grade of HCC [21–23], while the results of these methods for HCC grading vary, and the costs of liver-specific agents are too high to be suitable for most HCC patients. Texture analysis based on arterial phase contrast-enhanced MR images was reported to evaluate the grade of HCC [24]; however, the case number in the study was very limited, and the results lacked validation. To the best of our knowledge, no studies have determined whether non-contrast-enhanced MRI radiomics features could be used to predict HCC grade. Therefore, the aim of this study was to investigate the value of non-contrast-enhanced MRI-based radiomics signatures to preoperatively predict HCC grade.

Materials and methods

Patients

This is a retrospective study for which ethical approval was obtained. The inclusion criteria were as follows: (1) patients who underwent surgical resection for pathologically confirmed HCC with an available histological report of HCC; (2) patients who underwent liver MRI within 1 week before operation; (3) patients who received no previous treatment, such as radiofrequency ablation, transcatheter arterial chemoembolisation (TACE), liver resection or percutaneous ethanol injection; and (4) the image quality met the requirement of analysis (clearly image without artefact in more than three slices and the lesion visible on the transverse plane). In total, 170 patients at our institute were retrospectively recruited between February 2012 and December 2016, consisting of 141 males and 29 females, with a median age of 55 years (range 25 to 74 years). One hundred fifty-six patients were infected with hepatitis B, and 14 patients did not have hepatitis B. The data for 170 patients were divided into two groups, namely, a training dataset (125 patients; 104 males [83.2%] and 21 females [16.8%], with a median age of 53 years [range 25 to 71 years]) and a test dataset (45 patients; 37 males [82.22%] and 8 females [17.78%], with a median age of 57 years [range 28 to 74 years]).

HCC histological grading

The histological grading data were retrieved from archived clinical histology reports, in which the histological grades of HCC tumours were noted. Low-grade tumours correspond to Edmondson grades I, I–II and II, and high-grade tumours correspond to Edmondson grades II–III, III, III–IV and IV [25].

MRI protocol and feature extraction

MR images were acquired with a 3.0-T MRI scanner (Discovery MR750, 3.0 T, GE Healthcare) with an eight-channel phase array coil that covered the entire liver. Baseline MRI included fast spoiled gradient-recalled echo T1-weighted imaging (WI) and periodically rotated overlapping parallel lines with enhanced reconstruction fat-suppression fast spin-echo T2WI. The detailed parameters of the MR sequences used are shown in Table 1.

Both T1WI and T2WI images were retrieved from a picture archiving and communication system (PACS, Carestream).

Table 1 Magnetic resonance imaging sequences and parameters

Sequence	FSPGR-TIWI	Propeller-FSE-FS-T2WI
TR/TE (ms)	180/2.1	3333–7058/83
FA	80	110
Section thickness (mm)	7	7
Matrix size	320 × 192	320 × 320
Bandwidth (Hz/pixel)	83.33	83.33
Field of view (cm)	36–40	36–40
Acquisition time (s)	19	148
Echo train length	1	26–32
No. of excitations	1	2

TR repetition time, *TE* echo time, *FA* flip angle, *FSPGR-TIWI* fast spoiled gradient-recalled echo T1-weighted image, *Propeller-FSE-FS-T2WI* periodically rotated overlapping parallel lines with enhanced reconstruction fat-suppression fast spin-echo T2-weighted image

The MR images were loaded into the ITK-SNAP software for manual segmentation (open source software; http://www.itk-snap.org), and a three-dimensional (3D) region of interest (ROI) that covered the whole tumour was delineated on both the axial T1WI and T2WI images on each slice respectively segmented by a radiologist with over 10 years of experience in abdominal imaging. The procedure is highlighted in Fig. 1.

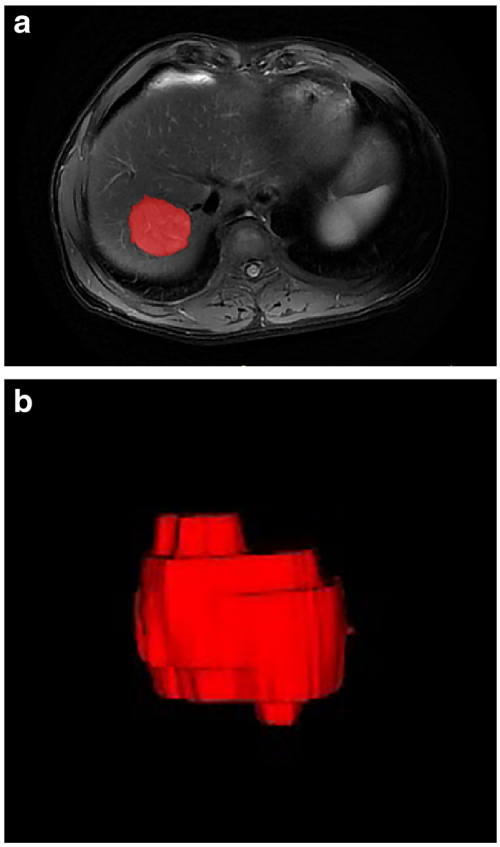

Fig. 1 **a** Delineation of the lesion using the ITK-SNAP software. **b** Generation of a 3D ROI

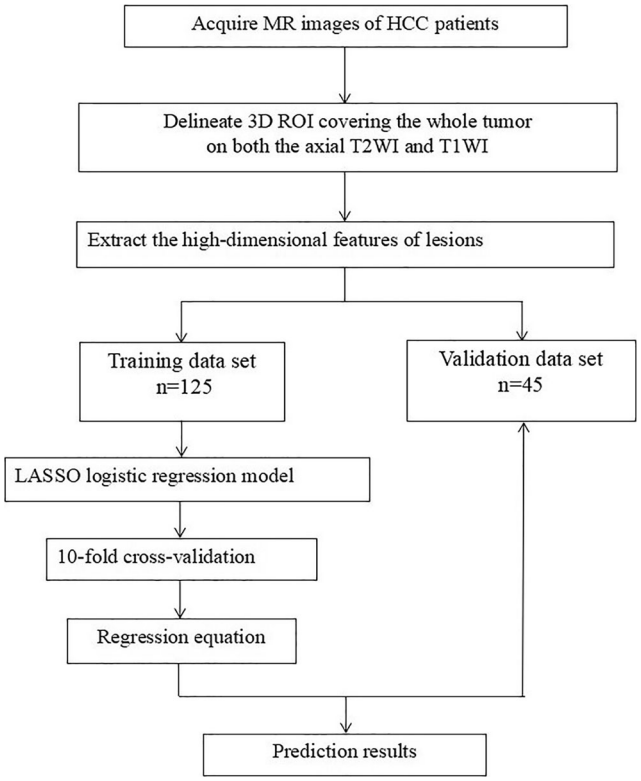

Fig. 2 Flow chart of the study

A total of 656 3D features from primary tumours were extracted, in which 328 features were based on T1WI and 328 features were based on T2WI. The features were divided into four groups: grey features (group 1), shape features (group 2), texture features (group 3) and wavelet features (group 4). The radiomics feature extraction methodology and the imaging traits are described in detail in Supplementary information 1.

Feature selection, radiomics signature construction and model training

Because the extracted features are high dimensional, the least absolute shrinkage and selection operator (LASSO) logistic

Table 2 Characteristic of HCC patients corresponding to the training and test datasets

Characteristic	Training dataset	Test dataset	*p* value
Sex (no. [%])			
Male	104 (83.2%)	37 (82.22%)	0.881
Female	21 (16.8%)	8 (17.78%)	
Age (years, median [range])	53 (25, 71)	57 (28, 74)	0.428
Stage (no. [%])			
High grade	70 (56%)	25 (55.56%)	0.894
Low grade	55 (44%)	20 (44.44%)	

P value < 0.05 indicates a significant difference in patient characteristic between the training and test datasets

HCC hepatocellular carcinoma

Table 3 Rad-scores for the training and test datasets

Rad-score	High-grade HCC Median (IQR)	Low-grade HCC Median (IQR)	*p* value
Based on T1WI			
Training dataset	0.4923 (0.2068 to 0.6847)	− 0.002311 (− 0.2035 to 0.2737)	< 0.0001
Test dataset	0.4298 (− 0.00231 to 0.6877)	− 0.1032 (− 0.5899 to 0.2781)	0.0194
Based on T2WI			
Training dataset	0.5268 (0.2505 to 0.9539)	− 0.1935 (− 0.6472 to 0.3074)	< 0.0001
Test dataset	0.4163 (− 0.08090 to 0.7208)	− 0.2091 (− 1.2217 to 0.1249)	0.0112
Based on T1WI and T2WI			
Training dataset	0.7079 (0.2714 to 1.1129)	− 0.1482 (− 0.8746 to 0.2948)	< 0.0001
Test dataset	0.6458 (− 0.1144 to 0.9932)	− 0.09459 (− 1.4707 to 0.2028)	0.0057

P value < 0.05 indicates a significant difference in the median Rad-scores between high-grade and low-grade HCC patients

IQR interquartile range

regression model, which is suitable for the regression of high-dimensional data, was used to select the most useful features from the primary data in the training dataset to solve the multicollinearity problem and construct the prediction model. The radiomics score (Rad-score) was calculated for each patient by using the linear combination of selected features multiplied by their respective coefficients. A 10-fold cross-validation was applied for training and selecting the optimal model for the pathological grading of HCC. The detail procedures are described in Supplementary information 2.

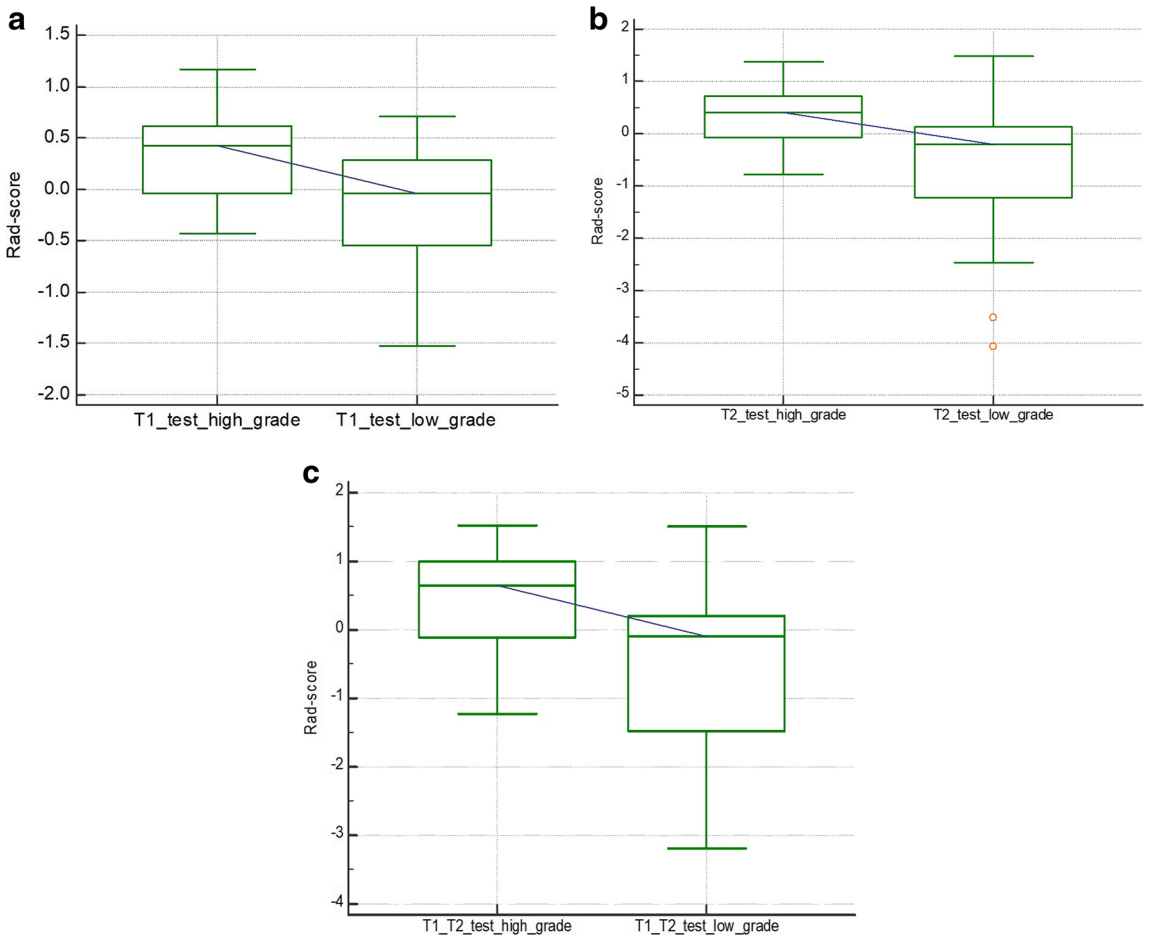

Fig. 3 Boxplots of Rad-scores in HCC patients. **a**–**c** Medians of the Rad-scores of high-grade cases based on T1WI (**a**), T2WI (**b**) and combined T1WI and T2WI (**c**) are higher than those of low-grade cases in the test dataset

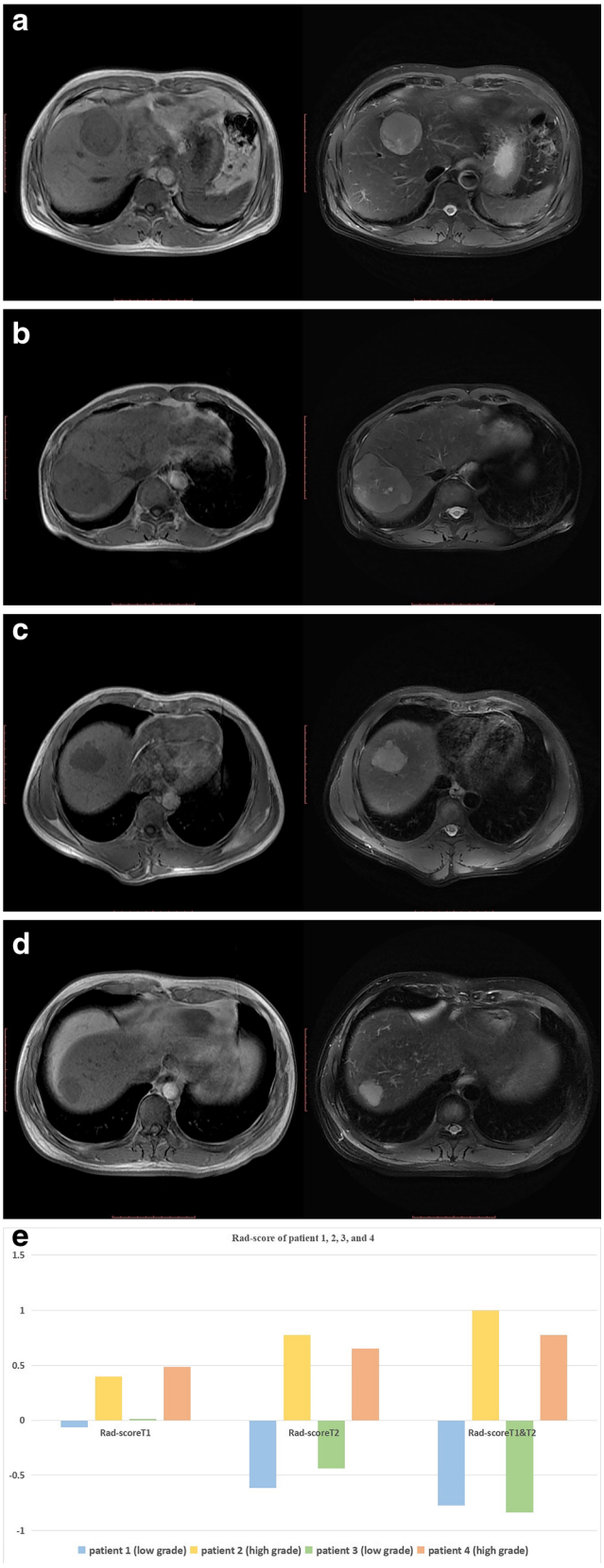

Fig. 4 Images based on T1WI and T2WI of patients with high-grade and low-grade HCC and the respective Rad-scores. **a** Patient 1, male, 60 years old, with Edmondson grade I–II (low-grade) HCC; Rad-scores based on T1WI, T2WI and combined T1WI and T2WI were − 0.0619, − 0.61134 and − 0.77037, respectively. **b** Patient 2, male, 65 years old, with Edmondson grade III (high-grade) HCC; Rad-scores based on T1WI, T2WI and combined T1WI and T2WI were 0.39853, 0.776079 and 0.999876, respectively. **c** Patient 3, male, 47 years old, with Edmondson grade II (low-grade) HCC; Rad-scores based on T1WI, T2WI and combined T1WI and T2WI were 0.013299, − 0.43544 and − 0.83285, respectively. **d** Patient 4, male, 45 years, with Edmondson grade II–III (high-grade) HCC; Rad-scores based on T1WI, T2WI and combined T1WI and T2WI were 0.485025, 0.653283 and 0.777851, respectively. **e** Rad-scores of patients 1, 2, 3 and 4 based on T1WI, T2WI and combined T1WI and T2WI

Predictive ability of the radiomics signature

The model assessed in the training dataset was applied to the test dataset. The areas under the receiver operating characteristic (ROC) curves (AUCs) along with 95% confidence intervals (CIs) and standard errors were analysed by the DeLong test in the MedCalc (Version 16.2.0, https://www.medcalc.org) software, and the cutoff value was selected according to the Youden index to determine the corresponding sensitivity and specificity. The AUCs were used to assess the predictive ability of the model. The process is outlined in Fig. 2.

Predictive ability of the clinical model and the combined model

A clinical prediction model was built to include age, sex, tumour size, alpha fetoprotein (AFP) level, history of hepatitis B, hepatocirrhosis, portal vein tumour thrombosis, portal hypertension and pseudocapsule based on a logistic regression model. Then, a combined model integrating the radiomics signature and all clinical information was built based on the logistic regression model. The predictive ability of the clinical model and the combined model was assessed with ROC curves generated and associated classification measures (AUC, sensitivity, specificity and accuracy).

Results

Clinicopathologic characteristics of patients

The clinicopathologic characteristics of patients whose data were classified into the training and test datasets are shown in Table 2. There were no differences between the training dataset and the test dataset in terms of age, sex or clinicopathologic characteristics (all $p > 0.05$).

Radiomics signature construction

In total, 656 features were extracted from MR images (328 features from T1WI and 328 from T2WI images). Based on T1WI, T2WI and combined T1WI and T2WI, 14, 18 and 20 features were selected, respectively, using the LASSO logistic regression model. The equation used to calculate the Rad-score for each patient was as follows:

$$\text{Rad-score} = \text{constant} + \text{coefficients} \times \text{features}$$

and the detailed parameters of the equation are shown in Supplementary information 3.

Predictive ability of radiomics signature (models)

A significant difference was observed between the median of the radiomics signature between high-grade and low-grade cases in both the training dataset ($p < 0.05$) and the test dataset ($p < 0.05$) (Table 3 and Figs. 3 and 4). The radiomics signatures based on T1WI and T2WI images performed well for the discrimination of high-grade patients from low-grade patients, with an average AUC of 0.712 and 0.722 in the test dataset (Fig. 5a, b; Table 4). The radiomics model from the combined T1WI and T2WI images displayed an AUC of 0.742 (95% CI 0.590 to 0.861) in the test dataset (Fig. 5c).

Predictive ability of the clinical model and the clinical model combined with the radiomics signatures

The AUC of the clinical model was 0.600 in the test dataset. The predictive ability (sensitivity, specificity and accuracy) of the clinical model is shown in Table 4. The predictive performance of the clinical model for the classification of high-grade vs. low-grade HCC cases in the test datasets is presented as ROC curves and described in Fig. 5d.

The combined model with clinical factors and radiomics signatures (based on T1WI images, T2WI images and combined T1WI and T2WI images) demonstrated AUCs of 0.742 (95% CI 0.590 to 0.861), 0.786 (95% CI 0.638 to 0.894) and 0.800 (95% CI 0.654 to 0.904), respectively, for the test dataset (Fig. 6a–c).

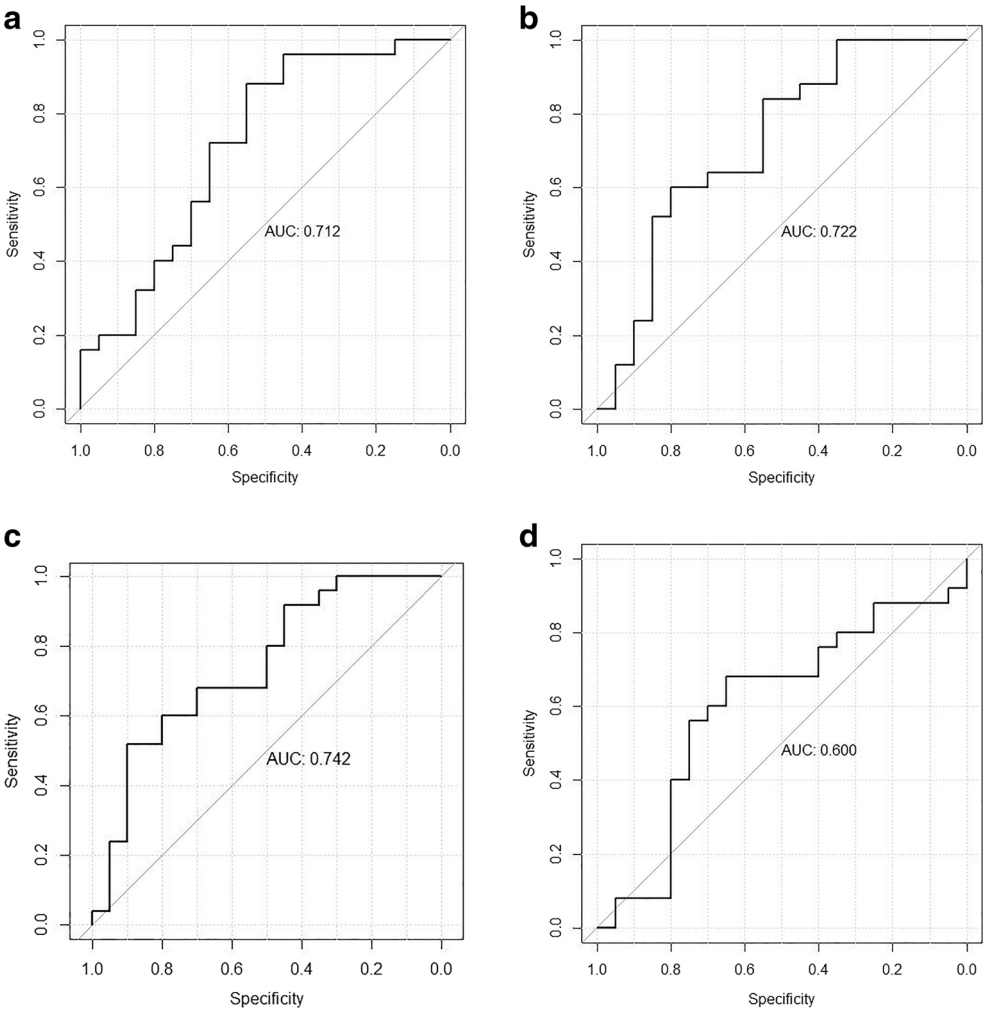

Fig. 5 ROC curves of the radiomics signatures and the clinical model in the test dataset. **a** The ROC curve of the radiomics signature based on T1WI for the test dataset; the AUC was 0.712. **b** The ROC curve of the radiomics signature based on T2WI for the test dataset; the AUC was 0.722. **c** The ROC curve of the radiomics signature based on combined T1WI and T2WI for the test dataset; the AUC was 0.742. **d** The ROC curves of the clinical model for the test dataset; the AUC was 0.600

Table 4 Predictive performance of the radiomics signature, the clinical model and the combined model

Method	Training dataset ($n = 125$)						Test dataset ($n = 45$)				
	Cutoff	Sensitivity (%)	Specificity (%)	Accuracy (%)	AUC (95% CI)	*p* value	Sensitivity (%)	Specificity (%)	Accuracy (%)	AUC (95% CI)	*p* value
LASSO (T1WI)	0.324313309	68.57	78.18	72.48	0.812 (0.732 to 0.876)	< 0.0001	52	75	62.22	0.712 (0.558 to 0.837)	0.0091
LASSO (T2WI)	0.108565067	81.43	63.64	73.6	0.804 (0.723 to 0.869)	< 0.0001	64	70	66.67	0.722 (0.568 to 0.845)	0.0059
LASSO (T1 + T2)	0.222519212	78.57	69.09	74.4	0.829 (0.752 to 0.891)	< 0.0001	72	65	68.89	0.742 (0.590 to 0.861)	0.0076
Clinical	0.5	81.16	54.55	69.45	0.794 (0.713 to 0.862)	< 0.0001	68	45	57.78	0.600 (0.443 to 0.743)	0.2670
Clinical + LASSO (T1)	0.219203525	78.57	72.37	75.36	0.8314 (0.754 to 0.892)	< 0.0001	68	75	71.11	0.742 (0.590 to 0.861)	0.0016
Clinical + LASSO (T2)	0.151388444	75	78.18	76.4	0.872 (0.801 to 0.925)	< 0.0001	70	75	72.22	0.786 (0.638 to 0.894)	0.0001
Clinical + LASSO (T1 + T2)	−0.868829854	95.71	70.91	84.4	0.909 (0.844 to 0.953)	0.0001	85	65	76.11	0.800 (0.654 to 0.904)	< 0.0001

95% CI 95% confidence interval, *AUC* area under the curve

As for the combined LASSO logistic regression models, both the AFP level and the radiomics signature were meaningful in classifying high-grade and low-grade HCC ($p < 0.05$) (Table 5).

Discussion

Radiomics has been shown to be useful in staging in lung and head and neck cancer, the prediction of survival of oropharyngeal squamous cell carcinoma and the determination of prognostic biomarkers of distant metastasis in lung adenocarcinoma patients [8, 26, 27]. In this study, we described a radiomics signature using non-contrast-enhanced MR images. The radiomics signatures based on T1WI and T2WI images were separately extracted, and three regression equations, which were used to calculate Rad-score, were obtained by a LASSO regression model, a 14-feature-based T1WI radiomics signature, an 18-feature-based T2WI radiomics signature and a 20-feature-based combined T1WI and T2WI signatures to test the discrimination of high-grade from low-grade HCC. Our results showed that the radiomics signature based on non-contrast-enhanced MR (T2WI or T1WI) images could successfully categorise HCC tumours into high-grade and low-grade cases in both the training dataset ($p < 0.05$) and the test dataset ($p < 0.05$). This indicates that T1WI or T2WI images could reflect the heterogeneity of tumours and radiomics features can be used to distinguish tiny signal differences in tumours.

Additionally, we also assessed the predictive values of the radiomics signature model (based on T1WI, T2WI and combined T1WI and T2WI images), the clinical model and the combined clinical and radiomics signature model (radiomics signature based on T1WI, T2WI and combined T1WI and T2WI images). Our results demonstrated that the radiomics signature based on T1WI or T2WI images showed similar performance in the prediction of the HCC grade (with AUCs of 0.712 and 0.722 in the test dataset). However, the clinical model showed the lowest AUC of 0.600 in the test dataset, while the combined clinical model and radiomics signature (based on combined T1WI and T2WI images) showed the highest AUC of 0.800 in the test dataset. Our results were very consistent with those from the study of Liang et al on radiomics signature-based grading on colorectal cancer [19], but the combined model in our study was more effective than that for colorectal cancer (with an AUC of 0.719 in the test dataset). This result may be related to the different tumour types having different heterogeneities.

Zhou et al [24] reported that texture features indexed by the mean value and grey-level run-length non-uniformity (GLN) based on Gd-DTPA-enhanced MR images were associated with the pathological grade of HCC (with AUCs of 0.827–

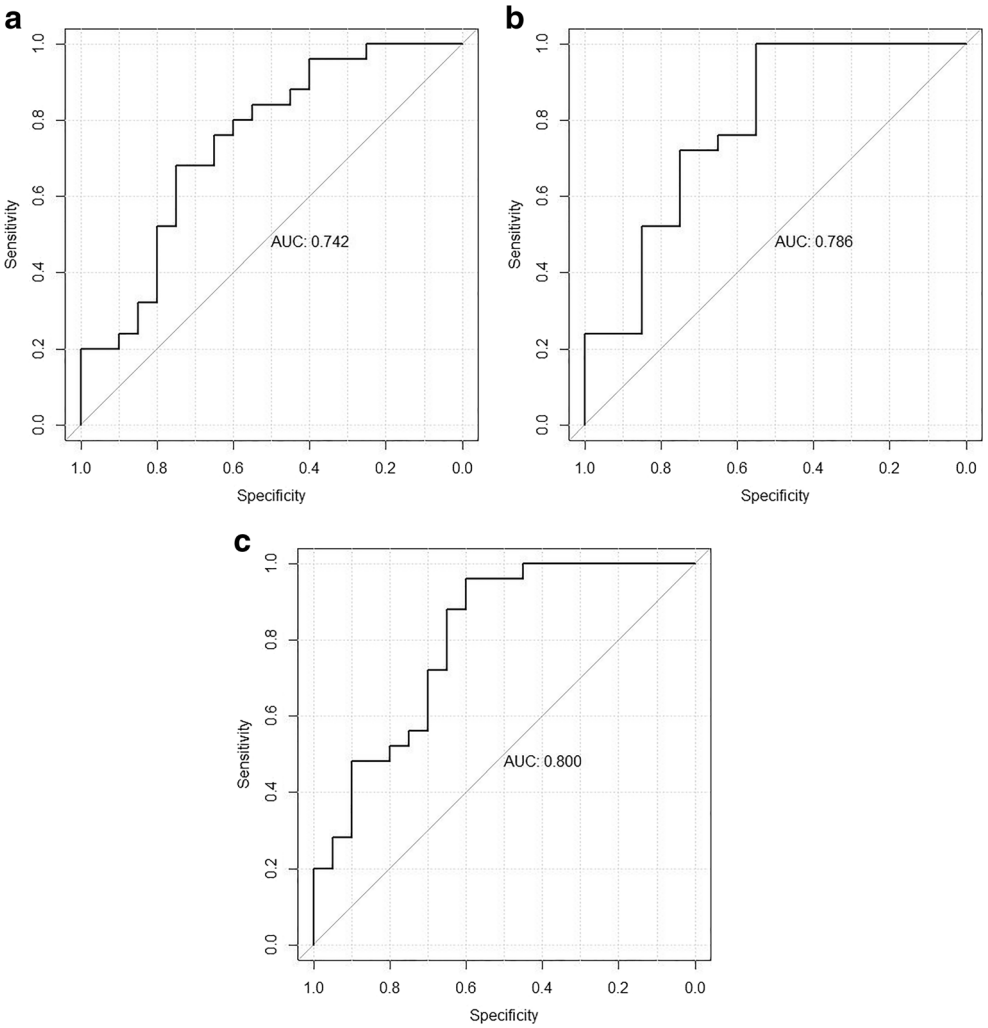

Fig. 6 ROC curves of the combined model. **a**–**c** The ROC curves of the combined T1WI-based radiomics signature and clinical model (**a** the AUC was 0.742 for the test dataset), the combined T2WI-based radiomics signature and clinical model (**b** the AUC was 0.786 for the test dataset) and the combined T1WI- and T2WI-based radiomics signatures and clinical model (**c** the AUC was 0.800 for the test dataset)

0.918), and their results were higher than ours. This may be related to enhanced MR images providing more information about tumour heterogeneity. However, only texture features were analysed in 46 HCC patients, which limited the comprehensive assessment of tumour heterogeneity compared with that achievable with radiomics signatures; additionally, the

Table 5 Preoperative prediction models of HCC stage

Constant and variables	Clinical model combined with radiomics signature		
	Coefficient	Odds ratios (95% CI)	*p* value
(Intercept)	− 1.62296	0.197314 (0.002069364, 15.46645799)	0.47184
Sex	0.25197	1.286557 (0.312187843, 5.351018269)	0.724723
Age	0.008593	1.00863 (0.953834931, 1.067860919)	0.763147
Area	− 0.00865	0.991384 (0.978776522, 1.003666023)	0.17116
Hepatitis B	− 0.81439	0.442908 (0.068233682, 2.490051132)	0.368815
AFP	1.60718	4.988721 (1.55812206, 17.70259494)	0.008811*
Pseudocapsule	0.369264	1.44667 (0.348626767, 6.320018507)	0.613113
Portal vein tumour thrombus	1.828037	6.22166 (1.139032241, 43.03709302)	0.055424
Hepatocirrhosis	− 0.33644	0.714312 (0.080615757, 5.828646879)	0.753226
Portal hypertension	0.957269	2.604574 (0.889554499, 8.029800585)	0.085092
Radiomics	2.52892	12.53996 (4.898494867, 39.15938992)	1.56E-06*

The combined model showing the results of a multivariate analysis of preoperative factors

95% CI 95% confidence interval

*p value < 0.05

case number was very limited, and the data lacked further test, which may have led to a possible risk of data overfitting.

In the combined model identified in our study, both the AFP level and radiomics signature were independent factors that could discriminate between high-grade and low-grade HCC ($p = 0.008811$ and $p = 0.00000156$, respectively). In previous studies, AFP levels were significant predictors of overall and disease-free survival in univariate analysis of HCC patients without microvascular invasion (MVI) [28] and of long-term HCC risk in patients with chronic hepatitis B (CHB) [29] and were independent risk factors associated with pathological grade, progression and survival [30], which was consistent with the results of our study.

However, there are some limitations in the current study. First, the number of HCC cases was limited, and the HCC tumours were divided into low-grade and high-grade cases instead of using the Edmondson grades. Thus, the validity of our findings may have been impaired. Therefore, more cases are needed for future studies. Second, in our study, most patients had a history of hepatitis B, and the group of patients was relatively homogeneous; thus, further research is needed to determine if our findings are reproducible in more heterogeneous liver diseases such as hepatitis C-related liver diseases and alcohol-related cirrhosis. Third, other MRI sequences, such as DWI and contrast-enhanced imaging, were not used in our study, and these might be useful in HCC grading. Thus, the images of these sequences should also be incorporated in future studies.

In conclusion, radiomics signatures based on T1WI and T2WI images may be useful for predicting the histological grade of HCC. A combination of clinical factors with the radiomics signatures can help distinguish high-grade HCC tumours from low-grade HCC tumours.

Funding The authors state that this work has not received any funding.

Compliance with ethical standards

Guarantor The scientific guarantor of this publication is Dapeng Shi.

Conflict of interest The authors of this manuscript declare no relationships with any companies, whose products or services may be related to the subject matter of the article.

Statistics and biometry No complex statistical methods were necessary for this paper.

Informed consent Written informed consent was obtained from all subjects (patients) in this study.

Ethical approval Institutional Review Board approval was obtained.

Methodology
- Retrospective
- Diagnostic or prognostic study
- Performed at one institution

References

1. Njei B, Rotman Y, Ditah I, Lim JK (2015) Emerging trends in hepatocellular carcinoma incidence and mortality. Hepatology 61: 191–199
2. El-Serag HB (2012) Epidemiology of viral hepatitis and hepatocellular carcinoma. Gastroenterology 142:1264–1273
3. Torre LA, Bray F, Siegel RL, Ferlay J, Lortet-Tieulent J, Jemal A (2015) Global cancer statistics, 2012. CA Cancer J Clin 65:87–108
4. Sasaki A, Kai S, Iwashita Y, Hirano S, Ohta M, Kitano S (2005) Microsatellite distribution and indication for locoregional therapy in small hepatocellular carcinoma. Cancer 103:299–306
5. Ng IO, Lai EC, Fan ST, Ng MM, So MK (1995) Prognostic signifcance of pathologic features of hepatocellular carcinoma: a multivariate analysis of 278 patients. Cancer 76:2443–2448
6. Okusaka T, Okada S, Ueno H et al (2002) Satellite lesions in patients with small hepatocellular carcinoma with reference to clinicopathologic features. Cancer 95:1931–1937
7. Bruix J, Sherman M (2005) Management of hepatocellular carcinoma. Hepatology 42:1208–1236
8. Parmar C, Leijenaar RT, Grossmann P et al (2015) Radiomic feature clusters and prognostic signatures specific for lung and head & neck cancer. Sci Rep 5:11044
9. Lambin P, Rios-Velazquez E, Leijenaar R et al (2012) Radiomics: extracting more information from medical images using advanced feature analysis. Eur J Cancer 48:441–446
10. Kumar V, Gu Y, Basu S et al (2012) Radiomics: the process and the challenges. Magn Reson Imaging 30:1234–1248
11. Goh V, Ganeshan B, Nathan P, Juttla JK, Vinayan A, Miles KA (2011) Assessment of response to tyrosine kinase inhibitors in metastatic renal cell cancer: CT texture as a predictive biomarker. Radiology 261:165–171
12. Ganeshan B, Goh V, Mandeville HC, Ng QS, Hoskin PJ, Miles KA (2013) Non-small cell lung cancer: histopathologic correlates for texture parameters at CT. Radiology 266:326–336
13. Ng F, Ganeshan B, Kozarski R, Miles KA, Goh V (2013) Assessment of primary colorectal cancer heterogeneity by using whole-tumor texture analysis: contrast-enhanced CT texture as a biomarker of 5-year survival. Radiology 266:177–184
14. Zhang H, Graham CM, Elci O et al (2013) Locally advanced squamous cell carcinoma of the head and neck: CT texture and histogram analysis allow independent prediction of overall survival in patients treated with induction chemotherapy. Radiology 269:801–809
15. Yip C, Landau D, Kozarski R, Ganeshan B, Thomas R, Michaelidou A et al (2014) Primary esophageal cancer: heterogeneity as potential prognostic biomarker in patients treated with definitive chemotherapy and radiation therapy. Radiology 270: 141–148
16. Liu S, Liu S, Ji C et al (2017) Application of CT texture analysis in predicting histopathological characteristics of gastric cancers. Eur Radiol 27:4951–4959
17. Ganeshan B, Abaleke S, Young RC, Chatwin CR, Miles KA (2010) Texture analysis of non-small cell lung cancer on unenhanced computed tomography: initial evidence for a relationship with tumour glucose metabolism and stage. Cancer Imaging 10:137–143
18. Ganeshan B, Skogen K, Pressney I, Coutroubis D, Miles K (2012) Tumour heterogeneity in oesophageal cancer assessed by CT texture analysis: preliminary evidence of an association with tumour metabolism, stage, and survival. Clin Radiol 67:157–164
19. Liang CS, Huang YQ, He L et al (2016) The development and validation of a CT-based radiomics signature for the preoperative discrimination of stage I-II and stage III-IV colorectal cancer. Oncotarget 7:31401–31412

20. Ayuso C, Rimola J, Garcia-Criado A (2012) Imaging of HCC. Abdom Imaging 37:215–230
21. Nasu K, Kuroki Y, Tsukamoto T, Nakajima H, Mori K, Minami M (2009) Diffusion-weighted imaging of surgically resected hepatocellular carcinoma: imaging characteristics and relationship among signal intensity, apparent diffusion coefficient, and histopathologic grade. AJR Am J Roentgenol 193:438–444
22. Nishie A, Tajima T, Asayama Y et al (2011) Diagnostic performance of apparent diffusion coefficient for predicting histological grade of hepatocellular carcinoma. Eur J Radiol 80:e29–e33
23. Kogita S, Imai Y, Okada M et al (2010) Gd-EOB-DTPA-enhanced magnetic resonance images of hepatocellular carcinoma: correlation with histological grading and portal blood flow. Eur Radiol 20:2405–2413
24. Zhou W, Zhang LJ, Wang KX et al (2017) Malignancy characterization of hepatocellular carcinomas based on texture analysis of contrast-enhanced MR images. J Magn Reson Imaging 45:1476–1484
25. Edmondson HA, Steiner PE (1954) Primary carcinoma of the liver. A study of 100 cases among 48,900 necropsies. Cancer 7:462–503
26. Coroller TP, Grossmann P, Hou Y et al (2015) CT-based radiomic signature predicts distant metastasis in lung adenocarcinoma. Radiother Oncol 114:345–350
27. Leijenaar RT, Carvalho S, Hoebers FJ et al (2015) External validation of a prognostic CT-based radiomic signature in oropharyngeal squamous cell carcinoma. Acta Oncol 54:1423–1429
28. Zhou L, Rui JA, Zhou WX, Wang SB, Chen SG, Qu Q (2017) Edmondson-Steiner grade: a crucial predictor of recurrence and survival in hepatocellular carcinoma without microvascular invasion. Pathol Res Pract 213:824–830
29. Chung JW, Jang ES, Kim J et al (2017) Development of a nomogram for screening of hepatitis B virusassociated hepatocellular carcinoma. Oncotarget 8:106499–106510
30. Bai DS, Zhang C, Chen P, Jin SJ, Jiang GQ (2017) The prognostic correlation of AFP level at diagnosis with pathological grade, progression, and survival of patients with hepatocellular carcinoma. Sci Rep 7:12870